Aquaculture 599 (2025) 742199

Contents lists available at ScienceDirect

Aquaculture

journal homepage: www.elsevier.com/locate/aquaculture

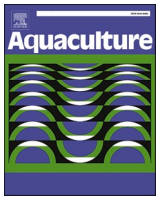

Mechanism of hypoxia tolerance improvement in hybrid fish Hefang bream

Ming Wen [1], Chunchun Zhu [1], Yuhua Tang [1], Hong Zhang, Zheng Liu, Siyu Wang, Min Tao, Li Hu, Wenting Rao, Shengnan Li, Dingbing Gong, Shi Wang, Shaojun Liu [*]

State Key Laboratory of Developmental Biology of Freshwater Fish, Engineering Research Center of Polyploid Fish Reproduction and Breeding of the State Education Ministry, College of Life Sciences, Hunan Normal University, Changsha 410081, Hunan, People's Republic of China

ARTICLE INFO

Keywords:
Hypoxia tolerance
Hybrid fish
Transcriptome
Metabolome
Gills

ABSTRACT

Hybrid breeding can combine advantageous genes from different species to generate new strains. Our laboratory has cultivated a hybrid fish called Hefang bream (HF) by hybridization between topmouth culter (*Culter alburnus*) and blunt snout bream (*Megalobrama amblycephala*, BSB). In aquaculture practice, it has shown stronger adaptability to low oxygen. To reveal the mechanism of hypoxia tolerance improvement of HF, we applied transcriptomics, metabolomics, and combined transcriptomics and metabolomics analysis. In this study, a comparison of hypoxic tolerance ability between HF and BSB showed that the tolerance to low oxygen of HF increased by 33.3 % compared to BSB. The transcriptome results showed that 1085 and 792 upregulated genes, 558 and 530 downregulated genes were screened out in HF and BSB after hypoxia treatment respectively. In HF, the KEGG pathway mainly involved the HIF-1 signaling pathway and glycolysis/glycogenesis. However, in BSB it mainly involved in the HIF-1 signaling and FoxO signaling pathway. The transcriptional metabolic association analysis results showed that the differentially expressed genes (DEGs) and differential metabolites were enriched in the pathway of ABC transporter protein and dicarboxylic acid metabolism in both HF and BSB. In addition, DEGs and differential metabolites were also enriched in lipid metabolism and purine metabolism in HF and enriched in ether lipid metabolism, arachidonic acid metabolism, arginine and proline metabolism pathways in BSB. Finally, we screened 8 candidate genes related to low oxygen response in fish (*egln3, im_7150988, klhl35, myl1, znf395a, hif-1 α n, epor, and eno1a*). In summary, we found the tolerance to low oxygen of HF was significantly ($P < 0.05$) improved compared to BSB, and a group of genes related to hypoxia tolerance were screened out.

1. Introduction

Hypoxia is a common natural phenomenon in fishery caused by temperature fluctuations, low photosynthetic activity, and low or stagnant water flow, which is more common in spring and summer (Li et al., 2022a). Research has shown that low oxygen in water would negatively affect the behavior, growth, physiological metabolism, and immune response of fish (Abdel-Tawwab et al., 2019; Saetan et al., 2020). For instance, in low oxygen water bodies, the swimming ability and speed of fish will be relatively reduced (Zhang et al., 2012). When the dissolved oxygen level is 4 mg/L, there will be a floating head phenomenon (Zhu et al., 2013). Crucian carp (*Carassius carassius*) can induce gill plate proliferation under low oxygen conditions, resulting in a significant increase in gill surface area (Sollid et al., 2003). Moreover, hypoxia can even lead to the extinction of low oxygen sensitive species (Karim et al., 2003). Therefore, the impact and losses to the aquaculture industry caused by hypoxia are great.

Fish have also developed various strategies to adapt to hypoxic environments during their long-term evolution, and their tolerance to hypoxia varies greatly (Bickler and Buck, 2007). The process of adaption to hypoxic stress in fish is very complex, including changing tissue morphology, regulating cell metabolism, and inducing hypoxia tolerant factors to adapt to hypoxic environments. The gill of fish can be reshaped in response to changes in oxygen content (Dabruzzi and Bennett, 2014). In low oxygen environment, fish will initiate special biological processes and molecular mechanisms to effectively store and utilize oxygen by regulating the expression of key genes (Rimoldi et al., 2012). Hypoxia stimulates aerobic glycolysis by regulating messenger RNA and targeting microRNA (Wang et al., 2018), such as hypoxia inducible factor 1 (HIF-1) and monocarboxylate transporter (MCTs). In addition,

* Corresponding author.
E-mail address: lsj@hunnu.edu.cn (S. Liu).
[1] These authors contributed equally to this work.

https://doi.org/10.1016/j.aquaculture.2025.742199
Received 3 August 2024; Received in revised form 19 January 2025; Accepted 21 January 2025
Available online 23 January 2025

hypoxia can also induce cell apoptosis to adapt to the low oxygen environment (Arend et al., 2011).

Blunt snout bream (*Megalobrama amblycephala*, BSB) is a herbivorous fish that is one of the most important economic fish with an annual output of more than 700,000 tons in the past 5 years in China (Li et al., 1993; Wen et al., 2022). BSB is a fish species that is sensitive to hypoxia. Short periods of hypoxia (less than 2 h) at room temperature (below 0.5 mg O_2/L) can be fatal (Li et al., 2015; Shen et al., 2010). Our laboratory has carried out genetic improvement for BSB by hybridizing female BSB and male topmouth culter (*Culter alburnus*, TC) to obtain hybrid fish of BSB (♀) × TC (♂) (BT), and backcross it with male parent BSB to obtain hybrid fish [BSB (♀) × TC (♂)] × BSB (♂) (BTB) (Li et al., 2022b; Ren et al., 2019; Xiao et al., 2014). Then, a new hybrid fish was obtained by the second round of backcross between female BSB and male BTB, named Hefang Bream (HF) (Gong et al., 2021a). The appearance of HF is similar to the blunt snout bream, and HF has higher muscle protein levels and lower muscle carbohydrate levels than BSB (Gong et al., 2021a). In aquaculture practice, we have found that the HF showed a stronger ability to low oxygen, and its floating head rate was low at lower dissolved oxygen conditions. However, the genetic mechanism related to its hypoxic tolerance is still unclear.

Transcriptomics is to study gene expression at the RNA level globally and provides information on differentially expressed genes and gene functions (Wang et al., 2009). Metabolomics explains the metabolic processes that occur in organisms after stimulation or destruction by providing information on the types and concentration changes of metabolites. In fish, liver tissue transcriptome profiles have been used to study the molecular mechanisms associated with hypoxia tolerance (Boswell et al., 2009; Li et al., 2015; Liao et al., 2013; Olsvik et al., 2013). In recent years, the exploration of genetic mechanisms related to stress responses in aquatic organisms, such as hypoxia tolerance, has been carried out through a combination of multiple omics approaches, such as kuruma shrimp (*Marsupenaeus japonicus*) (Ren et al., 2020), tilapia mossambica (*Oreochromis mossambicus*) (Ma et al., 2021), pufferfish (*Takifugu fasciatus*) (Wen et al., 2019), manila clam (Nie et al., 2020) and oyster (*Crassostrea hongkongensis*) (Li et al., 2017).

In fish, the gill is one of the most complex organs, playing a role in functions of gas oxygen and carbon dioxide exchange, water balance, ion regulation, and immune defense (Rombough, 2007). The gill of some fish can be reshaped according to changes in water DO levels (Dhillon et al., 2013). For example, in zebrafish (*Danio rerio*) interlayer cell apoptosis can be activated to increase the contact area with water to promote oxygen absorption (Onukwufor and Wood, 2020). The gill remodeling induced by hypoxia is reversible. And when fish return to a normal oxygen environment from hypoxia, the gill structure will also return to normal (Sollid and Nilsson, 2006). The plasticity of gill morphology contributes to enhancing the ability to absorb oxygen in water, thereby prolonging the survival time of fish (Nilsson, 2007). These studies indicate that fish adapt to low oxygen levels in water by reshaping gill morphology under hypoxic conditions. However, the mechanisms by which gill adapts to the fluctuated oxygen concentration in water at the molecular and cellular levels worth further study.

In this study, we compared the ability of low oxygen tolerance of HF and its parent BSB, as well as the morphological changes of gill under normoxic and hypoxic conditions. The comprehensive study was conducted by combining transcriptomics and metabolomics of gill tissue to investigate the differences in gene expression and metabolites during hypoxia stress within/between the two fish species. Finally, the candidate genes related to hypoxia tolerance were screened out, and the differences in genetic and metabolic regulation between HF and BSB under hypoxia stress were analyzed.

2. Materials and methods

2.1. Experimental fish

The experimental fish was obtained from Hunan Fish Genetics and Breeding Center, State Key Laboratory of Freshwater Fish Developmental Biology, Hunan Normal University, China. Fish work was performed in strict accordance with the recommendations in the Guidelines for the Care and Use of Laboratory Animals of the National Advisory Committee for Laboratory Animal Research in China and approved by the Animal Care Committee of Hunan Normal University (Permit Number: 4237). Before the experiment began, the fish were domesticated in an 80 L water-recirculating tank with DO 7.5 ± 0.5 mg/L, 25 ± 1 °C, and pH 7.6 ± 0.2 for 15 days. During the domestication period, fresh commercial feed, with 3 mm diameter size and ~ 28 % protein content, was fed twice a day, and residual bait was promptly removed. Oxygen, temperature, and pH were measured using a Portable multifunctional water quality detector (Smart sensor AR8407).

2.2. Hypoxia treatment

During June, HF and BSB were selected with uniform size, normal activities, and health. For each species, fish were placed into 80 L water tanks with 10 fish for one tank (hypoxic groups) and 10 fish for the control group (normoxic group). The dissolved oxygen in the water was regulated with a system by filling nitrogen and pumping oxygen in the water. An oxygen monitor was used to monitor the dissolved oxygen concentration in the water in real-time. The dissolved oxygen concentration was maintained at 7.5 ± 0.5 mg/L in the normoxic group, and the dissolved oxygen level in the hypoxic group was maintained at 6.0 mg/L for 1 h, subsequently decreased to 3.0 mg/L for 30 min and held for 30 min, then decreased to 1.5 mg/L for 30 min and held for 30 min, subsequently decreased to 1.0 mg/L for 30 min and held for 30 min, finally held to 0.5 mg/L for 30 min and held for 30 min (Wu et al., 2017). The dissolved oxygen concentration and time were observed and recorded when fish showed loss of equilibrium. The critical oxygen tension for loss of equilibrium (LOE_{crit}) was calculated using Brett's equation (Brett, 1964):

$$LOE_{crit} = [O_2]_{2i} - \left(\frac{t_i}{t_{ii}}\right)[O_2]_{2ii}$$

In this equation, $[O_2]_{2i}$ is the minimum oxygen content at which fish can maintain equilibrium throughout the entire process; t_i is the time it takes for the fish to lose equilibrium at the final $[O_2]_{2i}$; t_{ii} is the time maintained for each $[O_2]_{2i}$; $[O_2]_{2ii}$ is the decrease in oxygen tension with each increase (0.5 mg /L).

2.3. Sample collection and blood analysis

For each species, six fish were sampled when the fish lost their balance during hypoxia treatments, meanwhile six experimental fish from the normoxic group were randomly selected for sampling. Before sampling, tricaine methanesulfonate (MS-222, Sigma) with a concentration of 0.30 mg/L was used to anesthetize experimental fish (Gong et al., 2020). Gill tissues were fixed in Bouin's solution for histological analysis. In addition, 6 samples of the gill tissue from each group were temporarily stored in liquid nitrogen and then transferred to −80 °C for storage for subsequent RNA extraction, library construction, transcriptome sequencing, and metabolomics analysis.

For each species, three fish from normoxic and hypoxic groups were respectively selected for blood extraction. After anesthesia, blood was extracted from the tail vein. Blood sample was collected in an EDTA-k2 anticoagulant tube for the detection of blood physiological indicators such as red blood cell count (RBC), white blood cell count (WBC), hemoglobin (Hb), and hematocrit (HCT). Blood indicators were detected

using Mindray Veterinary Fully Automatic Hematology Analyzer (BC-2800vet).

2.4. Histological and light microscopy analysis

The gill tissues from 5 samples of each species were fixed in Bouin's solution for 24 h. The fixed sample was dehydrated with an alcohol gradient, was transparent with xylene, embedded in paraffin, and finally sliced. The slice thickness was approximately 5 μm, then stained with hematoxylin eosin (HE), sealed with neutral gum, and observed and photographed under an optical microscope (Tao et al., 2018). The gill filaments were measured using the software ImageJ (Saito and Mori, 2023), recording the length, thickness, spacing, and interlayer cell mass height of the gill segments (Matey et al., 2008).

2.5. RNA extraction, library construction, and transcriptome sequencing

The total RNA of gill tissue was extracted using a TRIzol reagent. The concentration and purification of the extracted RNA were detected using Nanodrop2000. The integrity of RNA was detected using agarose gel electrophoresis and the RIN value was measured using Agilent2100. Subsequently, according to the special structure of mRNA with ployA tail at the 3 "end, it could be isolated from the total RNA using magnetic beads with Oligo (dT). Then adding fragmentation buffer, mRNA was randomly broken, and small fragments around 300 bp were isolated using magnetic bead. Single-stranded cDNA using mRNA as a template was synthesized with the kit of reverse transcriptase, followed by double-stranded synthesis to form a stable double-stranded structure. The double-stranded cDNA had cohesive ends, which were complemented with End Repair Mix to form a flat end. Then, the 'A' base was added to the 3" end. Finally, sequencing was performed on the Illumina Novaseq 6000 sequencing platform (Gong et al., 2021b).

2.6. Metabolite extraction and LC-MS/MS analysis

For the control group and treatment group, metabolites were extracted from the gill tissue of each sample. The extraction of metabolites was carried out with traditional methods using a 1 mL mixture of acetonitrile methanol solvent (acetonitrile/methanol/water = 2:2:1). After adding the extraction solvent, sample was vortexed for 30 s, heated at 45 Hz for 4 min, sonicated for 5 min, and stored in ice water. Then sample was homogenized and ultrasound treated three times. The obtained solution was incubated at −20 °C for 1 h and refrigerated centrifuged at 13500*g* for 15 min. The supernatant was stored at −80 °C and transferred for LC-MS/MS analysis. Sample quality control was conducted by mixing an equal amount of supernatant to analyze the reproducibility of each group (Wen et al., 2019).

2.7. Association analysis of transcriptome and metabolome

Combining transcriptome and metabolomic analysis was to determine regulatory pathways involving differentially expressed genes and metabolites. Using the Cytoscape software (Shannon et al., 2003), the relationships between significantly differentially expressed genes (DEGs) and differential metabolites were mapped into interaction networks, which provided rich and comprehensive information to reveal the molecular mechanisms of response to hypoxia stress (Sun et al., 2021).

2.8. Statistical analysis

As the data was not normally distributed, a non-parametric test, Kruskall-Wallis test, was applied for data analysis. And the Dunn's test was selected for the post-hoc test. Data statistics were implemented using GraphPad prism (Lv et al., 2023).

3. Results

3.1. Comparison of hypoxic tolerance ability between HF and BSB

Through a comparative experiment on the low oxygen tolerance of the HF and BSB, the results showed that the LOE_{crit} value of BSB was relatively higher than the LOE_{crit} value of HF (Fig. 1). Compared to BSB, the average low oxygen tolerance of HF increased by 33.3 %, and its advantage in low oxygen tolerance was significant ($P < 0.05$).

3.2. Effects of hypoxia on the morphology of gill

Our results showed that after acute hypoxia treatment, the gill segments of HF and BSB extend outward, with a significant increase in length compared to their control group. The gill segments were significantly thinner, and their interlayer space was increased. The height of interlayer cell mass (ILCM) was significantly decreased. The change of gill morphology in HF was more pronounced than those of BSB (Fig. 2). After hypoxia treatment, the length of gill segments in HF and BSB was significantly longer than those in the normoxic group ($P < 0.05$). The Breadth of gill segments after hypoxia treatment was significantly smaller than that of the normoxic group ($P < 0.05$). The average interval between layers in HF and BSB after hypoxia treatment was significantly higher than that of the normoxia group ($P < 0.05$). In addition, the height of interlayer cell mass (ILCM) between gill segments in HF and BSB were significantly lower than that of the normoxic group (Table 1).

3.3. Effects of hypoxia on blood physiological indicators

Hypoxia tolerance could induce the change of the blood physiological indicators in HF and BSB. After hypoxia treatment, the RBC of HF and BSB were increased, while the WBC and Hb were decreased compared to the normoxic group. However, the HCT of HF significantly was increased after hypoxia treatment, while the HCT of BSB was significantly decreased ($P < 0.05$) (Table 2).

3.4. Identification and functional enrichment of DEGs

The cDNA samples of the normoxic group and hypoxic group of HF and BSB were subjected to high-throughput sequencing on the Illumina Hiseq 6000 platform. A total of 84.36 Gb raw data was generated. After removing adapters, fuzzy nucleotides, and low-quality reads, clean data for each sample ranged from 6.24 Gb to 7.70 Gb, then clean data were analyzed for quality control. The base percentage of Q30 of all samples was above 95.03 %. High-quality transcriptome data provides a reliable

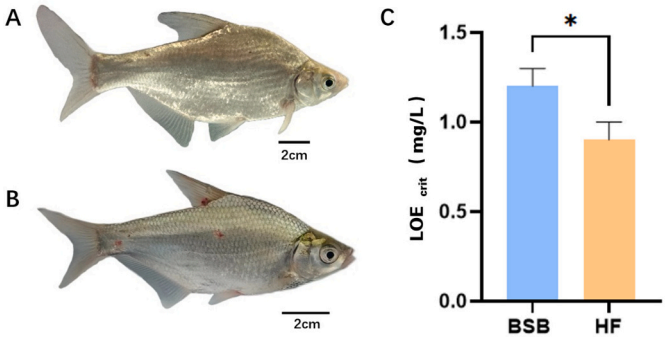

Fig. 1. The appearance of Hefang bream (HF) and Blunt snout bream (BSB) and comparative analysis of hypoxic tolerance between Hefang bream (HF) and Blunt snout bream (BSB).
(A) The appearance of Hefang bream (HF). (B) The appearance of Blunt snout bream (BSB). (C) Comparative analysis of hypoxia tolerance of Hefang bream (HF) and Blunt snout bream (BSB). Asterisk (*) indicated $P < 0.01$. *t*-test was used for data statistics.

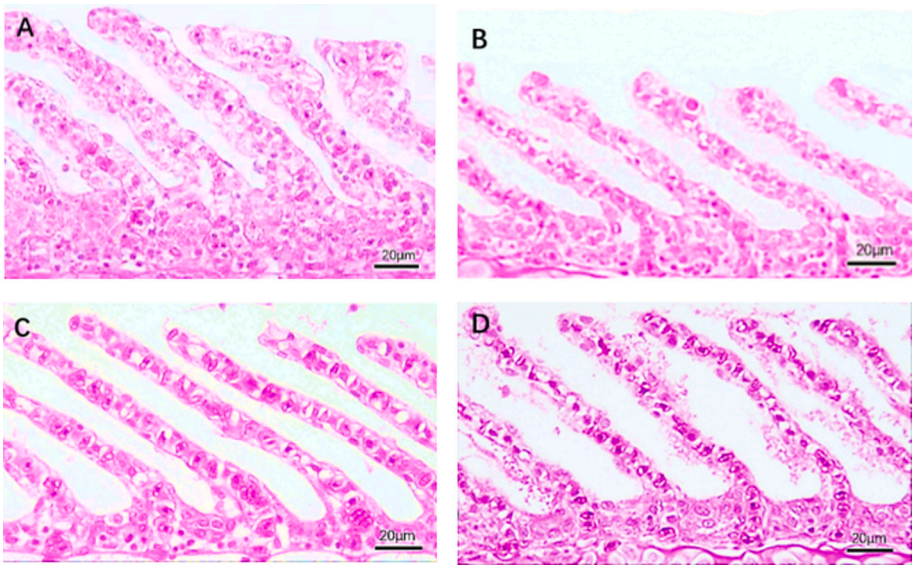

Fig. 2. Microstructure of gill tissue in hypoxic and normoxic groups of Hefang bream (HF) and Blunt snout bream (BSB).
(A) Gill from normoxic group of Hefang bream (HF). (B) Gill from normoxic group of Blunt snout bream (BSB). (C) Gill from hypoxic group of Hefang bream (HF). (D) Gill from hypoxic group of Blunt snout bream (BSB).

Table 1
Values of variables on gill lamella in control and hypoxic treatment groups.

	BSB		HF	
	Normoxia	Hypoxia	Normoxia	Hypoxia
Length of gill lamella (μm)	91.85 (87.79–96.09)^{d}	129.10 (124.69–130.96)^{b}	116.40 (113.37–120.47)^{c}	151.35 (150.78–153.72)^{a}
Breadth of gill lamella (μm)	11.38 (11.12–11.46)^{a}	8.19 (7.58–8.67)^{b}	13.55 (12.51–16.71)^{a}	7.43 (6.96–7.78)^{b}
Intervals of gill lamella (μm)	14.96 (14.51–16.59)^{c}	23.55 (21.02–25.55)^{a}	11.95 (10.92–12.56)^{d}	19.56 (18.26–20.43)^{b}
Height of ILCM (μm)	19.91 (17.65–21.32)^{b}	16.85 (15.74–17.28)^{bc}	36.35 (31.14–37.21)^{a}	16.09 (15.37–16.88)^{c}

Note: Different superscript letters for the same row indicate significant differences between groups ($P < 0.05$). Interlayer cell mass (ILCM); Blunt snout bream (BSB); Hefang bream (HF). Data presenting in each cell of the table are "median (first quartile - third quartile)". Dunn's test was used for data statistics.

Table 2
Blood physiological indicators in control and hypoxic treatment groups.

Indicators	BSB		HF	
	Normoxia	Hypoxia	Normoxia	Hypoxia
RBC /(10^{12}/mL)	1.06 (0.92–1.29)^{a}	2.03 (1.51–2.39)^{a}	1.64 (1.45–1.71)^{a}	1.76 (1.35–1.99)^{a}
WBC /(10^{9} /mL)	189.97 (181.97–197.46)^{a}	191.58 (151.06–207.03)^{a}	206.21 (204.29–209.02)^{a}	190.73 (157.67–206.70)^{a}
Hb /(10^{9} /mL)	102.39 (98.69–104.88)^{a}	111.56 (81.83–128.60)^{a}	116.14 (111.40–122.49)^{a}	98.60 (83.41–115.59)^{a}
HCT /%	19.17 (17.81–21.72)^{b}	25.75 (16.77–29.78)^{ab}	27.61 (26.46–29.16)^{a}	24.54 (20.38–28.16)^{ab}

Note: Different superscript letters for the same row indicate significant differences between groups ($P < 0.05$). Red blood cell count (RBC); White blood cell count (WBC); Hemoglobin (Hb); Hematocrit (HCT); Blunt snout bream (BSB); Hefang bream (HF). Data presenting in each cell of the table are "median (first quartile - third quartile)". Dunn's test was used for data statistics.

dataset for further analysis of the response to acute hypoxia of HF and its parent, BSB.

Comparative transcriptome analysis between the normoxic and hypoxic groups of HF showed a total of 1643 DEGs ($P < 0.05$ and $|\log2fc| > 1$), including 1085 upregulated genes and 558 downregulated genes. A total of 1322 DEGs ($P < 0.05$ and $|\log2fc| > 1$) between the normoxic and hypoxic groups of BSB was identified, including 792 upregulated genes and 530 downregulated genes (Fig. 3B). Taking the intersection of the two groups of DEGs, 428 genes were co-differentially expressed genes in both HF and BSB between hypoxic group and normoxic group (Fig. 3A). To visually display the DEGs between the two groups, we plotted a volcano plot to show the up-regulation (red dots) and down-regulation (blue dots) of genes in the acute hypoxia response of the two species (Fig. 3C, D). Furthermore, we identified significant DEGs in HF between control and hypoxia treatment groups, including *znf395a*, *egln3*, *myl1*, and *klhl35*. In BSB, the genes including *znf395a*, *egln3*, and *mknk2b* were significantly differentially expressed.

Through GO enrichment analysis of DEGs in BSB, it was found that DEGs are mainly enriched in biological processes related to hypoxia, such as cellular response to hypoxia (GO: 0071456), cellular response to decreased oxygen levels (GO: 0036294), response to decreased oxygen levels (GO: 0036293), and response to hypoxia (GO: 001666) (Fig. S1B). GO enrichment analysis of HF exhibited the DEGs mainly distributed in low oxygen-related processes, such as cellular response to hypoxia (GO: 0036294) Cellular response to decreased oxygen levels (GO: 0036294), in addition to myosin complexes (GO: 0016459), and biological regulation (GO: 065007) (Fig. S1A).

To understand the enrichment pathways of DEGs, the DEGs of HF and BSB were mapped to reference pathways in the KEGG database. Among the top 20 KEGG pathways of HF, they were mainly related to

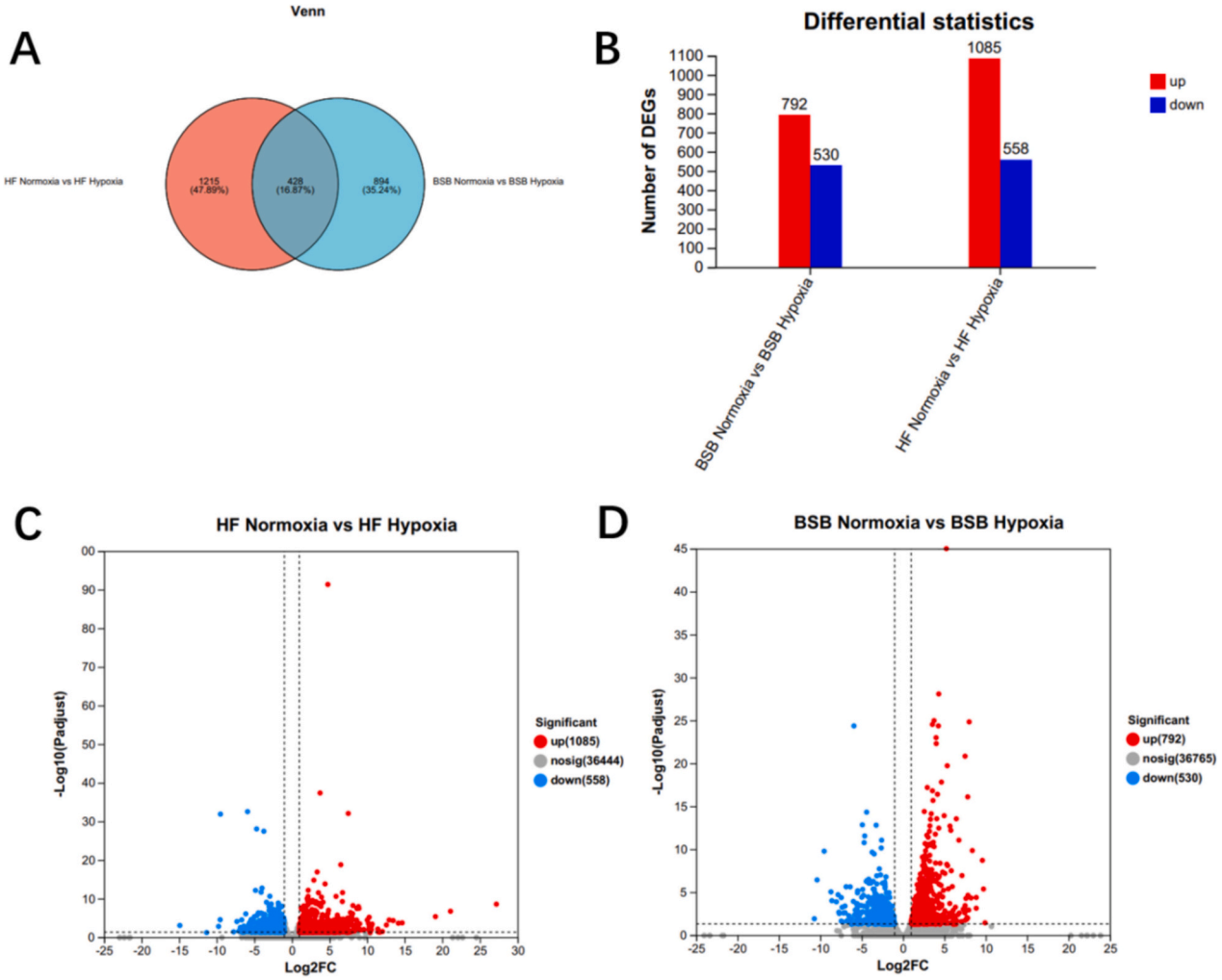

Fig. 3. Identification of DEGs in Hefang bream (HF) and Blunt snout bream (BSB) after hypoxia treatment.
(A) Venn plot showed common and specific DEGs in Hefang bream (HF) and Blunt snout bream (BSB), with red representing DEGs identified from Hefang bream (HF) and blue representing DEGs identified from Blunt snout bream (BSB). (B) Numbers of up- and down-regulated DEGs in Hefang bream (HF) and Blunt snout bream (BSB), with red representing upregulated genes and blue representing downregulated genes. (C) The volcano plot showed significantly DEGs in Hefang bream (HF) after hypoxia treatment. (D) The volcano plot showed significant DEGs in Blunt snout bream (BSB) after hypoxia treatment, with red and blue dots indicated upregulated and downregulated DEGs, and grey dots indicated no significant DEGs. (For interpretation of the references to colour in this figure legend, the reader is referred to the web version of this article.)

cancer-related pathways "pathways of cancer", "microRNA in cancer", as well as cardiovascular disease-related pathways "Hypertrophic cardiomyopathy", "arrhythmic right ventricular cardiomyopathy" and "myocardioconstriction". Therefore, it was reasonable to speculate that an acute hypoxic environment can aggravate the heart load of fish and cause disease. In addition, DEGs were also enriched in the "HIF-1 signaling pathway" and "Glycolysis/Glycogenesis" (Fig. S2A). Among the top 20 KEGG pathways of BSB, the differentially expressed genes were mainly involved in "the pathogenesis of cancer", "cytokine-cytokine receptor interaction", and "lipid and atherosclerosis". At the same time, the DEGs of BSB also enriched several important pathways related to hypoxia resistance, such as the "HIF-1 signaling pathway" and the "FoxO signaling pathway" (Fig. S2B).

3.5. *Metabolite identification and functional enrichment*

According to the quantitative analysis of metabolites, a total of 1559 positive-mode metabolites and 1657 negative-mode metabolites were obtained. The OPLS-DA analysis showed that the metabolic spectrums were well separated into different clusters in the two groups of HF and BSB (Fig. S2). To prevent the overfitting of the model, a replacement test based on 200 tests was used to verify the OPLS-DA model. The intercept values of positive mode and negative mode were low, indicating that the overfitting and reliability risk of the OPLS-DA model were low. Therefore, the OPLS-DA model in this study was stable and effective in identifying the metabolic differences between the two species responding to acute hypoxia. Using the threshold of variable important in projection (VIP) value more than 1 and *P* value less than 0.05, the metabolites with significant differences between the two groups were screened. The results showed that a total of 284 differential metabolites were detected between the HF hypoxia group and the normal oxygen group, among them 134 differential metabolites in cationic mode and 150 differential metabolites in anionic mode. In the cationic mode, compared with the normal oxygen group, 97 metabolites were up-regulated and 37 metabolites were down-regulated in the low oxygen group. In the anionic mode, 118 up-regulated and 32 down-regulated metabolites were identified in the hypoxic group compared with the normoxic group. A total of 369 differential metabolites were detected in BSB between hypoxic group and normoxic group with 205 differential metabolites in cationic mode and 164 differential metabolites in anionic mode. In the cationic mode, compared with normoxic group, 101 metabolites were up-regulated and 104 metabolites were down-regulated

in hypoxic group. In anionic mode, 72 up-regulated metabolites and 92 down-regulated metabolites were identified. Differential metabolites were visually presented in the volcano plots showing the difference between normoxic and hypoxic groups in HF and BSB (Fig. 4A, B).

Comparing the normoxic and hypoxic groups of HF, 30 significantly differential metabolites (SDMs) were obtained, of which 28 SDMs had higher concentrations in the hypoxic group than in the normal oxygen group. In BSB, 30 SDMs were obtained between the normoxic and hypoxic groups, with 19 SDMs exhibiting higher concentrations in the hypoxic group than in the normoxic group. Through KEGG enrichment analysis, 15 pathways of significant enrichment of SDMs were found between HF normoxic and hypoxic groups, including phenylalanine, tyrosine and tryptophan biosynthesis, glycine, serine and threonine metabolism, minoacyl-tRNA biosynthesis. There were also 15 pathways of significant enrichment of SDMs between BSB normoxic and hypoxic groups, including ether lipid metabolism, arginine biosynthesis, arginine and proline metabolism. SDMs were mainly enriched in amino acid metabolism-related pathways in both BSB and HF, and the also enriched in lipid metabolism-related pathways in BSB (Fig. 4C, D).

3.6. Correlation analysis of transcriptome and metabolome

We further integrated the transcriptome and metabolome using the correlation coefficient model, orthogonal production to late structure (O-PLS) model, and the KEGG Pathway model to screen relevant genes and metabolites. The first 50 metabolites and the first 200 genes were screened. And the Pearson correlation coefficient analysis was carried out using the screened differential metabolites and DEGs. The heat map of the correlation matrix showed the positive and negative correlation between metabolites and genes (Fig. S4).

In the KEGG pathway analysis, the common pathways of the two sets of DEGs and differential metabolites were analyzed. The results of enrichment pathway analysis of HF showed that the pathway was mainly related to four pathways including ABC transporter, lipid metabolism, dicarboxylic acid metabolism, and purine metabolism. The DEGs and differential metabolites of BSB were mainly enriched in five pathways including ABC transporter, dicarboxylic acid metabolism, ether lipid metabolism, arachidonic acid metabolism, arginine and proline metabolism (Fig. S5). Among them, enrichment pathways of ABC transporter, dicarboxylic acid metabolism, and Lipid metabolism were identified in both HF and BSB.

3.7. QPCR verification of DEGs

To verify the quality of RNA-seq data, we selected 8 DEGs that were related to hypoxia response enrichment pathways or significantly differentially expressed between hypoxic and normoxic groups, including egl-9 family hypoxia induction factor 3 (*egln3*), related plant

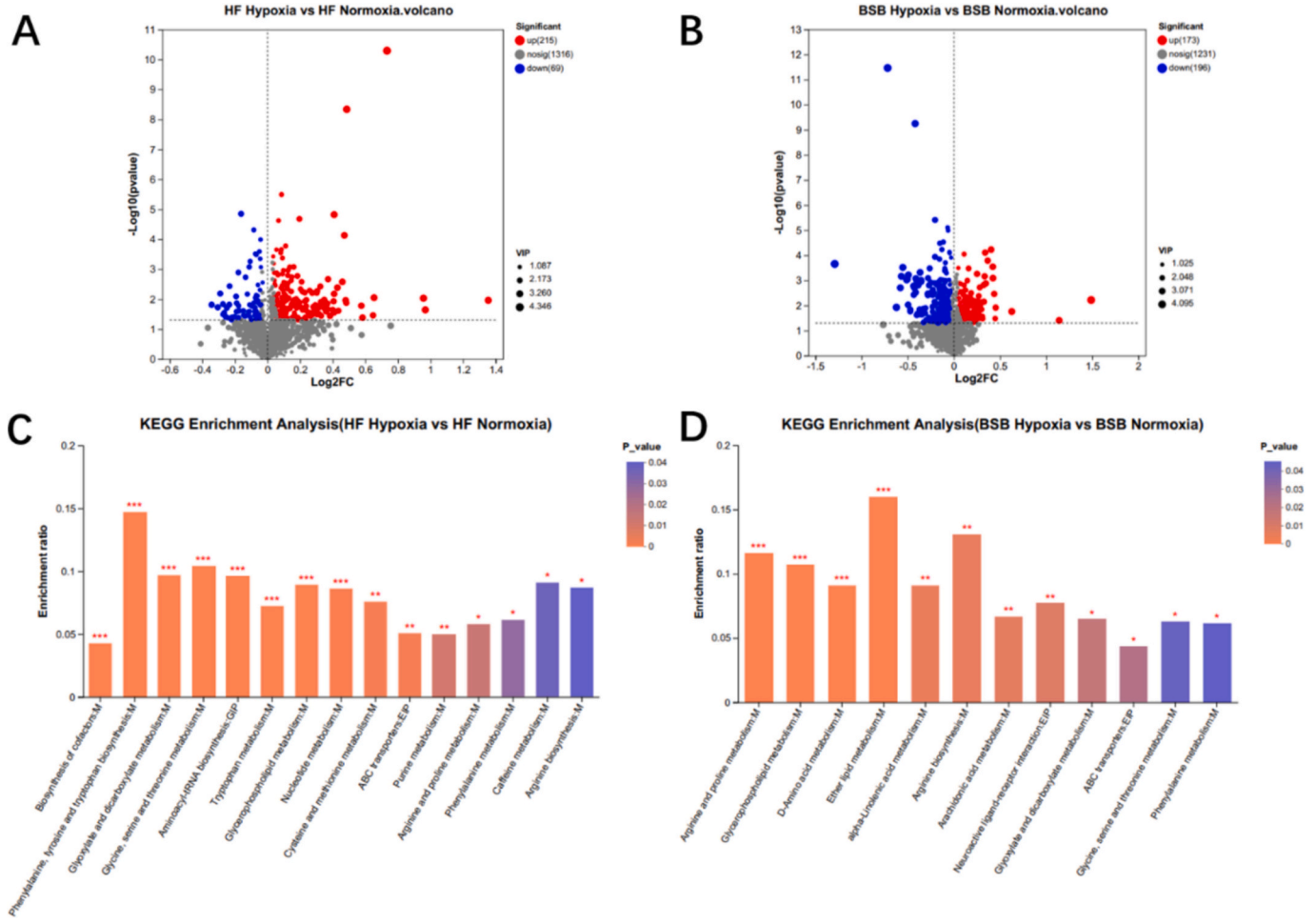

Fig. 4. Differential metabolites and KEGG enrichment analysis in Hefang bream (HF) and Blunt snout bream (BSB) after hypoxia treatment.
(A) The volcano plot of differential metabolites in Hefang bream (HF) after hypoxia treatment. (B) The volcano plot of differential metabolites in Blunt snout bream (BSB) after hypoxia treatment, the red and blue dots in the volcano plot represent up-regulated and down-regulated DMs, and the X and Y axis represent the log2 (FC) value and -log10 (P) value respectively. (C) KEGG enrichment analysis of Hefang bream (HF) DMs. (D) KEGG enrichment analysis of Blunt snout bream (BSB) DMs. (For interpretation of the references to colour in this figure legend, the reader is referred to the web version of this article.)

pathogenesis related protein 1 (*im_7150988*), kelch family Member 35 (*klhl35*), myosin light chain 1 alkaline bone rapid (*myl1*), zinc finger protein 395a (*znf395a*), hypoxia inducing factor 1αn (*hif-1αn*), erythropoietin receptor (*epor*), enolase 1a (α) transcription variant X1 (*eno1a*). And qPCR was conducted with three biological replicates and three technological replicates. QPCR results showed that after hypoxia treatment the gene expression levels of *egln3*, *myl1*, *znf395a*, *hif-1αn*, *epor* and *eno1a* were up-regulated in both BSB and HF. On the contrary, the gene expression levels of *im_7150988* and *klhl35* were down-regulated (Fig. 5). The qPCR data was consistent with the expression spectrum identified from RNA-seq, which indicates the reliability of transcriptome data.

4. Discussion

Fish evolved different mechanisms for adaptation to hypoxia stress in different species, and even among closely related species the adaptability to hypoxia stress is different (Gong et al., 2021b). BSB is an aquaculture important fish while it is sensitive to hypoxia. Hypoxia caused great harm to the culture of BSB. Previous studies have shown that genetic improvement of fish germplasm resources could enhance their ability to resistance. For example, using the technique of gynogenesis, it could improve the hypoxia tolerance of BSB (Gong et al., 2021a). In addition, a new BSB strain with higher tolerance to hypoxia stress was established using the population selection technique (Wu et al., 2020). Our laboratory had prepared HF, a hybrid fish, by hybridizing female BSB and male BTB. By comparison, it was found that the hypoxia tolerance of HF was 33.3 % higher than its original parent BSB. It showed that hybrid breeding can cultivate dominant species with strong stress resistance and provide important “seed chips” to promote the development of aquaculture.To further explore the mechanism of hypoxia tolerance, the dominant trait of hybrid fish, we conducted research related to hypoxia tolerance.

In this study, we found that after acute hypoxia treatment, the gill pieces of HF and BSB extended outward, the length increased significantly, the thickness of the gills became significantly thinner, and the spacing between the layers increased. This morphological change of gill increased the surface area of breathing, which was conducive to gas exchange and oxygen absorption. The thickness and layer spacing of HF were more significant than that of its original parent BSB, which was likely one of the reasons that HF was more resistant to low oxygen. Previous studies have shown that when dissolved oxygen dropped to a very low level, the gills of crucian carp changed such as gill interstitial withering and gill filaments extension to obtain more dissolved oxygen from the water environment. When the dissolved oxygen returned to normal level, its gill structure would gradually return to normal morphology (Sollid et al., 2003). And it is similar to our research results. These results showed that fish will change the shape of the gill to adapt to hypoxia and increase the contact area with oxygen to promote oxygen absorption and maintain metabolic requirements.

Blood is a key indicator of feedback that fish are affected by environmental factors. After hypoxia treatment, the RBC of BSB and HF increased significantly, and it might increase the blood’s ability to transport oxygen by increasing the amount of RBC in the blood. However, Hb showed a low concentration in the low oxygen condition, and the number of RBC changed more sensitively than Hb. The HCT of HF was significantly increased after hypoxia stress, while the HCT of BSB was significantly reduced. Compared with BSB, HF could also increase its adaptability to low oxygen by adjusting HCT.

After hypoxia treatment, using the analysis of gill transcriptomics, we identified a series of DEGs, including *egln3*, *myl1*, *im_7150988*, *klhl35*, *znf395a*, *hif-1αn*, *epor* and *eno1a*. And, the expression of up-regulated genes *egln3*, *myl1*, and *znf395a* was more significant in HF than in BSB, and the expression of down-regulated gene *im_7150988* was

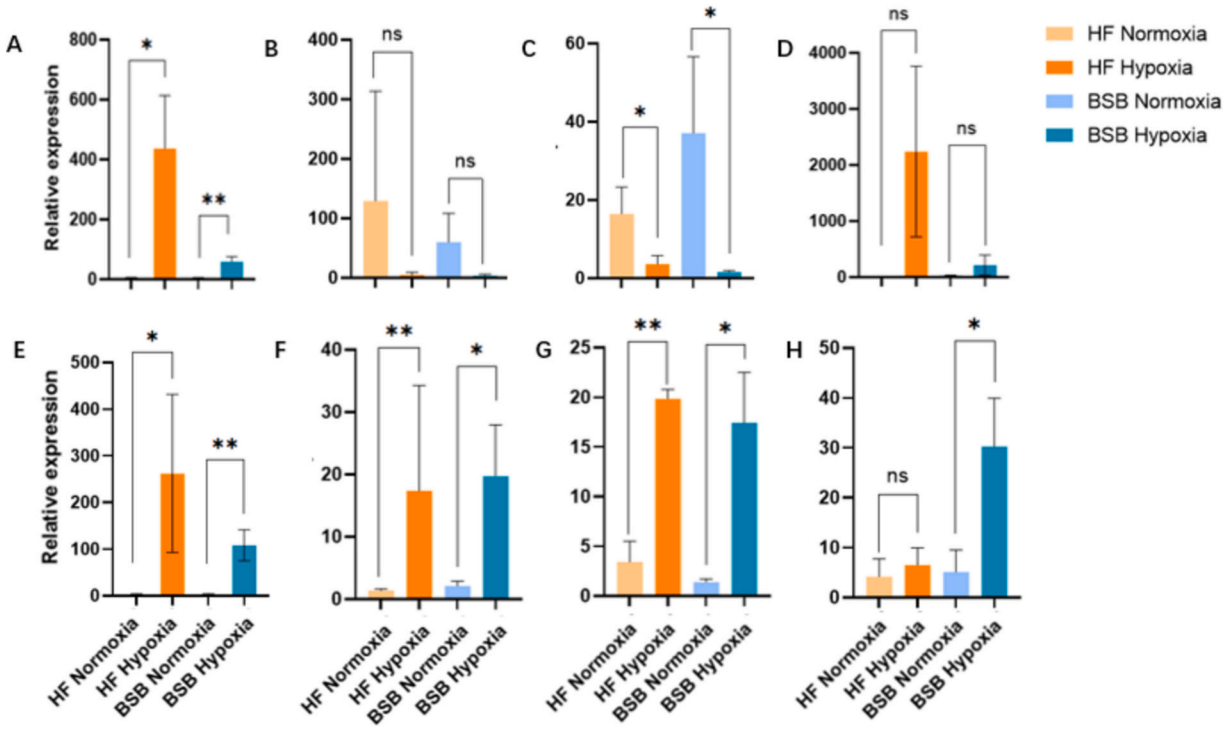

Fig. 5. QPCR validation of 8 significant DEGs identified from Hefang bream (HF) and Blunt snout bream (BSB) after hypoxia treatment.
(A) Egl-9 family hypoxia inducing factor 3 (*egln3*). (B) Related plant pathogenesis-related protein 1 (*im_7150988*). (C) Kelch family members 35 (klhl35). (D) Myosin, light chain 1, alkaline; bone, rapid (*myl1*). (E) Zinc finger protein 395a (*znf395a*). (F) Hypoxia inducing factor 1αn (*hif-1αn*). (G) Erythropoietin receptor (*epor*). (H) Enolase 1a, (α), transcript Variant X1 (*eno1a*). The asterisk (*) indicated a significant difference between the control group (normoxic group) and the treatment group (hypoxic group) ($p < 0.05$).The asterisk (**) indicated a significant difference ($p < 0.01$) between the control group and the treatment group, while ns indicated no significant difference between the two groups. t-test was used for data statistics.

more significant in HF than in BSB. It implied that the mechanism of hypoxia response of HF was more sensitive than BSB. Among them, *znf395a* in HF and BSB was the most significant gene. *Znf395a* was the direct target gene of the hypoxia induction factor hif-1α and the main regulatory factor of the hypoxia reaction. In the process of hypoxia regulation, elevated levels of *znf395a* could support inflammation and cancer by activating the target gene involved in the innate immune response (Jordanovski et al., 2013).

The HIF-1 signaling pathway is a key pathway in the process of hypoxia. Hypoxia induction factor 1 (*HIF-1*) is the main regulatory factor of the hypoxia signaling pathway (Li et al., 2015). It was composed of *hif-1α* and *hif-1β* subunits, which could merely express stably under hypoxia conditions. So far, more than 100 *HIF-1* downstream genes have been identified, which were involved in red blood cell production/iron metabolism, glucose metabolism, cell proliferation, angiogenesis, apoptosis, oxygen delivery, or hypoxia metabolism adaptation (Lundby et al., 2009). The transcriptomic results of this study showed that many key genes in the HIF-1 signaling pathway of HF and BSB including *Egln1*, *Egln2*, *Egln3*, *Hif1αα*, *Hif1l*, *Sl2a1b*, and *Vhl* were all up-regulated. And *Hif1αα* and *Hif1l* were expressed higher in HF than in BSB, while *Egln1*, *Egln2*, and *Egln3* were expressed lower in HF than in BSB. In addition, vascular endothelial growth factor A (*Vegfa*) was involved in the regulation of angiogenesis and oxygen transport (Chen et al., 2017), which was only significantly highly expressed in HF. The signaling pathway mediated by *HIF-1* was related to low-oxygen tolerance, and the difference in the amount of gene expression might be one of the reasons why the low-oxygen resistance of the HF was higher than that of BSB.

Studies have shown that in fish the anaerobic metabolism will be enhanced and aerobic metabolism will be inhibited at the early stage of acute hypoxia stress (Sun et al., 2020). In this study, we found that after the treatment of acute hypoxia stress, the up-regulated metabolites of HF and BSB were enriched in several important glucose metabolic pathways, including glycolysis/glycolysis and insulin signaling pathways. Glycolysis is the main way of anaerobic metabolism (Mizock, 1995). GAPDH is a multifunctional glycolytic enzyme (Camacho-Jiménez et al., 2018), which can catalyze the mutual conversion of 1,3-diphosphate glycerin and 3-phosphoglyceride for participating in DNA repair, membrane fusion and transport, RNA binding, autophagy, and other biological processes (Tristan et al., 2011). GAPDHS inactivation converts the intracellular carbohydrate breakdown process from glycolysis to the pentose phosphate pathway, leading to the production of NADPH and protecting cells from oxidative stress (Ralser et al., 2007). Phosphoenol pyruvate carboxykinase 1 (PCK1) can catalyze oxal acetic acid to produce phosphoenol pyruvate, releasing GDP and carbon dioxide. PCK1 is a speed-limiting enzyme that regulates glucose. It is involved in maintaining blood glucose levels and is considered indispensable for maintaining glucose homeostasis (Beale et al., 2003). Our results showed that after the hypoxia treatment of HF and BSB, the expression of PCK1 was up-regulated, which might accelerate the glucosantogenous pathway to regulate the metabolism of glucose in the cell. The expression of GAPDH was significantly upregulated in the HF, enhancing glycolysis to adapt to the low-oxygen environment. However, it was down-regulated in BSB, which may weaken the glycolysis pathway. The insulin signaling pathway plays an important role in blood glucose regulation. Insulin (INS) is a protein hormone secreted by islet B cells, which regulates energy metabolism, such as glucose and lipid metabolism. This signaling pathway is mainly transmitted by insulin receptors (INSR) and protein kinases. Our KEGG pathway enrichment showed that some up-regulated genes of HF and BSB were significantly enriched in the insulin signaling pathway to reduce hypoglycemia, inhibit glucose consumption, and thus inhibit glycogen decomposition.

5. Conclusion

In this study, we investigated the mechanism of hypoxia tolerance improvement of hybrid fish, HF, by comparing to its original parent BSB. We described the dynamics of gill morphology and blood indicators subject to hypoxia treatment. In addition, we identified a batch of key candidate genes responding to hypoxia stress. By combining transcriptome and metabolome, we identified some important pathways related to hypoxia response. In the future, it is worth of verifying these candidate genes' function in response to hypoxia and analyzing the network regulating mechanism. Our results provided a solid foundation for revealing the mechanism of the improvement of hypoxic tolerance in hybrid fish and promoting germplasm innovation of aquatic varieties.

Author statement

Shaojun Liu and Ming Wen conceived the project, designed the experiments and acquired funding. Chunchun Zhu analyzed transcriptome and metabolome sequencing data, modified this manuscript. Yuhua Tang, Hong Zhang, Zheng Liu conducted investigation. Siyu Wang helped in collecting samples and doing investigation. Min Tao modified this manuscript and acquired funding. Li Hu, Wenting Rao and Shengnan Li modified this manuscript. Dingbing Gong and Siyu Wang helped in collecting samples.

CRediT authorship contribution statement

Ming Wen: Writing – review & editing, Writing – original draft, Funding acquisition, Data curation, Conceptualization. **Chunchun Zhu:** Writing – review & editing, Writing – original draft, Visualization, Validation, Investigation, Data curation. **Yuhua Tang:** Investigation. **Hong Zhang:** Investigation. **Zheng Liu:** Investigation. **Siyu Wang:** Investigation. **Min Tao:** Writing – review & editing, Funding acquisition. **Li Hu:** Writing – review & editing. **Wenting Rao:** Writing – review & editing. **Shengnan Li:** Writing – review & editing. **Dingbing Gong:** Investigation. **Shi Wang:** Investigation. **Shaojun Liu:** Writing – review & editing, Writing – original draft, Supervision, Funding acquisition, Conceptualization.

Declaration of competing interest

The authors declare that they have no competing interests.

Data availability

Data will be made available on request.

Acknowledgements

This work was supported by the National Key R & D Program (2022YFD2400600/2022YFD2400604), the Natural Science Foundation of Hunan (Grant No. 2023JJ40433), the National Natural Science Foundation of China (Grant No. 32293252, U19A2040), the Training Program for Excellent Young Innovators of Changsha (Grant No. kq2107006), the Youth Science and Technology Talents Lifting Project of Hunan Province (Grant No. 2023TJ-N02).

Appendix A. Supplementary data

Supplementary data to this article can be found online at https://doi.org/10.1016/j.aquaculture.2025.742199.

References

Abdel-Tawwab, M., Monier, M.N., Hoseinifar, S.H., Faggio, C., 2019. Fish response to hypoxia stress: growth, physiological, and immunological biomarkers. Fish Physiol. Biochem. 45, 997–1013.

Arend, K.K., Beletsky, D., DePinto, J.V., Ludsin, S.A., Roberts, J.J., Rucinski, D.K., Scavia, D., Schwab, D.J., Höök, T.O., 2011. Seasonal and interannual effects of hypoxia on fish habitat quality in Central Lake Erie. Freshw. Biol. 56, 366–383.

Beale, E.G., Forest, C., Hammer, R.E., 2003. Regulation of cytosolic phosphoenolpyruvate carboxykinase gene expression in adipocytes. Biochimie 85, 1207–1211.
Bickler, P.E., Buck, L.T., 2007. Hypoxia tolerance in reptiles, amphibians, and fishes: life with variable oxygen availability. Annu. Rev. Physiol. 69, 145–170.
Boswell, M.G., Wells, M.C., Kirk, L.M., Ju, Z.L., Zhang, Z.P., Booth, R.E., Walter, R.B., 2009. Comparison of gene expression responses to hypoxia in viviparous (Xiphophorus) and oviparous (Oryzias) fishes using a medaka microarray. Comp. Biochem. Physiol. C 149, 258–265.
Brett, J.R., 1964. The respiratory metabolism and swimming performance of young sockeye salmon. J. Fish. Res. Board Can. 21, 1183–1226.
Camacho-Jiménez, L., Peregrino-Uriarte, A.B., Martínez-Quintana, J.A., Yepiz-Plascencia, G., 2018. The glyceraldehyde-3-phosphate dehydrogenase of the shrimp (Litopenaeus vannamei): molecular cloning, characterization and expression during hypoxia. Mar. Environ. Res. 138, 65–75.
Chen, B.-X., Yi, S.-K., Wang, W.-F., He, Y., Huang, Y., Gao, Z.-X., Liu, H., Wang, W.-M., Wang, H.-L., 2017. Transcriptome comparison reveals insights into muscle response to hypoxia in blunt snout bream (Megalobrama amblycephala). Gene 624, 6–13.
Dabruzzi, T.F., Bennett, W.A., 2014. Hypoxia effects on gill surface area and blood oxygen-carrying capacity of the Atlantic stingray, Dasyatis sabina. Fish Physiol. Biochem. 40, 1011–1020.
Dhillon, R.S., Yao, L.L., Matey, V., Chen, B.J., Zhang, A.J., Cao, Z.D., Fu, S.J., Brauner, C. J., Wang, Y.X.S., Richards, J.G., 2013. Interspecific differences in hypoxia-induced gill remodeling in carp. Physiol. Biochem. Zool. 86, 727–739.
Gong, D.B., Xu, L.H., Li, W.H., Shang, R.J., Chen, J.X., Hu, F.Z., Wang, S., Liu, Q.F., Wu, C., Zhou, R., Zhang, C., Tao, M., Wang, Y.Q., Liu, S.J., 2020. Comparative analysis of liver transcriptomes associated with hypoxia tolerance in the gynogenetic blunt snout bream. Aquaculture 523, 735163.
Gong, D., Xu, L., Liu, Q., Wang, S., Wang, Y., Hu, F., Wu, C., Luo, K., Tang, C., Zhou, R., Zhang, C., Tao, M., Wang, Y., Liu, S., 2021a. A new type of hybrid bream derived from a hybrid lineage of Megalobrama amblycephala (♀) × Culter alburnus (♂). Aquaculture 534, 736194.
Gong, D.B., Xu, L.H., Liu, Q.F., Wang, S., Wang, Y.D., Hu, F.Z., Wu, C., Luo, K.K., Tang, C. C., Zhou, R., Zhang, C., Tao, M., Wang, Y.Q., Liu, S.J., 2021b. A new type of hybrid bream derived from a hybrid lineage of (Megalobrama amblycephala)(♀) x (Culter alburnus)(♂). Aquaculture 534.
Jordanovski, D., Herwartz, C., Pawlowski, A., Taute, S., Frommolt, P., Steger, G., 2013. The hypoxia-inducible transcription factor ZNF395 is controlled by IκB kinase-signaling and activates genes involved in the innate immune response and cancer. PLoS One 8, e74911.
Karim, M.R., Sekine, M., Ukita, M., 2003. A model of fish preference and mortality under hypoxic water in the coastal environment. Mar. Pollut. Bull. 47, 25–29.
Li, S., Cai, W.Q., Zhou, B.Y., 1993. Variation in morphology and biochemical genetic markers among populations of blunt snout bream (Megalobrama amblycephala). Aquaculture 111, 117–127.
Li, F.G., Chen, J., Jiang, X.Y., Zou, S.M., 2015. Transcriptome analysis of blunt snout bream (Megalobrama amblycephala) reveals putative differential expression genes related to growth and hypoxia. PLoS One 10, e0142801.
Li, J., Zhang, Y.H., Mao, F., Tong, Y., Liu, Y., Zhang, Y., Yu, Z.N., 2017. Characterization and Identification of differentially expressed genes involved in thermal adaptation of the Hong Kong oyster (Crassostrea hongkongensis) by digital gene expression profiling. Front. Mar. Sci. 4.
Li, J., Zhang, G., Yin, D., Li, Y., Zhang, Y., Cheng, J., Zhang, K., Ji, J., Wang, T., Jia, Y., Yin, S., 2022a. Integrated application of multiomics strategies provides insights into the environmental hypoxia response in pelteobagrus vachelli muscle. Mol. Cell. Proteomics 21, 100196.
Li, S.N., Yang, X.Q., Fan, S.Y., Zhou, Z.F., Zhou, R., Wu, C., Gong, D.B., Wen, M., Wang, Y.Q., Tao, M., Liu, S.J., 2022b. Comparative analysis of muscle nutrient in two types of hybrid bream and native bream. Reproduct. Breed. 2, 71–77.
Liao, X.L., Cheng, L., Xu, P., Lu, G.Q., Wachholtz, M., Sun, X.W., Chen, S.L., 2013. Transcriptome analysis of crucian carp (Carassius auratus), an important aquaculture and hypoxia-tolerant species. PLoS One 8.
Lundby, C., Calbet, J.A.L., Robach, P., 2009. The response of human skeletal muscle tissue to hypoxia. Cell. Mol. Life Sci. 66, 3615–3623.
Lv, C., Chen, K., Zhu, L., 2023. Identification of key genes and potential mechanisms based on the autophagy regulatory network in intervertebral disc degeneration. Medicine 102, e33482.
Ma, J.L., Qiang, J., Tao, Y.F., Bao, J.W., Zhu, H.J., Li, L.G., Xu, P., 2021. Multi-omics analysis reveals the glycolipid metabolism response mechanism in the liver of genetically improved farmed Tilapia (GIFT, Oreochromis niloticus) under hypoxia stress. BMC Genomics 22.
Matey, V., Richards, J.G., Wang, Y.X., Wood, C.M., Rogers, J., Davies, R., Murray, B.W., Chen, X.Q., Du, J.Z., Brauner, C.J., 2008. The effect of hypoxia on gill morphology and ionoregulatory status in the Lake Qinghai scaleless carp, Gymnocypris przewalskii. J. Exp. Biol. 211, 1063–1074.
Mizock, B.A., 1995. Alterations in carbohydrate metabolism during stress: a review of the literature. Am. J. Med. 98, 75–84.
Nie, H.T., Wang, H.M., Jiang, K.Y., Yan, X.W., 2020. Transcriptome analysis reveals differential immune related genes expression in Ruditapes philippinarum under hypoxia stress: potential HIF and NF-κB crosstalk in immune responses in clam. BMC Genomics 21, 318.
Nilsson, G.E., 2007. Gill remodeling in fish - a new fashion or an ancient secret? J. Exp. Biol. 210, 2403–2409.
Olsvik, P.A., Vikeså, V., Lie, K.K., Hevroy, E.M., 2013. Transcriptional responses to temperature and low oxygen stress in Atlantic salmon studied with next-generation sequencing technology. BMC Genomics 14.
Onukwufor, J.O., Wood, C.M., 2020. Osmorespiratory compromise in zebrafish (Danio rerio): effects of hypoxia and acute thermal stress on oxygen consumption, diffusive water flux, and sodium net loss rates. Zebrafish 17, 400–411.
Ralser, M., Wamelink, M.M., Kowald, A., Gerisch, B., Heeren, G., Struys, E.A., Klipp, E., Jakobs, C., Breitenbach, M., Lehrach, H., Krobitsch, S., 2007. Dynamic rerouting of the carbohydrate flux is key to counteracting oxidative stress. J. Biol. 6, 10.
Ren, L., Li, W., Qin, Q., Dai, H., Han, F., Xiao, J., Gao, X., Cui, J., Wu, C., Yan, X., Wang, G., Liu, G., Liu, J., Li, J., Wan, Z., Yang, C., Zhang, C., Tao, M., Wang, J., Luo, K., Wang, S., Hu, F., Zhao, R., Li, X., Liu, M., Zheng, H., Zhou, R., Shu, Y., Wang, Y., Liu, Q., Tang, C., Duan, W., Liu, S., 2019. The subgenomes show asymmetric expression of alleles in hybrid lineages of Megalobrama amblycephala × Culter alburnus. Genome Res. 29, 1805–1815.
Ren, X.Y., Yu, Z.X., Xu, Y., Zhang, Y.B., Mu, C.M., Liu, P., Li, J., 2020. Integrated transcriptomic and metabolomic responses in the hepatopancreas of kuruma shrimp (*Marsupenaeus japonicus*) under cold stress. Ecotox. Environ. Safe 206.
Rimoldi, S., Terova, G., Ceccuzzi, P., Marelli, S., Antonini, M., Saroglia, M., 2012. HIF-1α mRNA levels in Eurasian perch (Perca fluviatilis) exposed to acute and chronic hypoxia. Mol. Biol. Rep. 39, 4009–4015.
Rombough, P., 2007. The functional ontogeny of the teleost gill: which comes first, gas or ion exchange? Comp. Biochem. Phys. A. 148, 732–742.
Saetan, W., Tian, C.X., Yu, J.W., Lin, X.H., He, F.X., Huang, Y., Shi, H.J., Zhang, Y.L., Li, G.L., 2020. Comparative transcriptome analysis of gill tissue in response to hypoxia in silver sillago (sillago sihama). Animals 10.
Saito, S., Mori, K., 2023. Detection and quantification of calcium ions in the endoplasmic reticulum and cytoplasm of cultured cells using fluorescent reporter proteins and ImageJ software. Bio-Protoc. 13, e4738.
Shannon, P., Markiel, A., Ozier, O., Baliga, N.S., Wang, J.T., Ramage, D., Amin, N., Schwikowski, B., Ideker, T., 2003. Cytoscape: a software environment for integrated models of biomolecular interaction networks. Genome Res. 13, 2498–2504.
Shen, R.J., Jiang, X.Y., Pu, J.W., Zou, S.M., 2010. HIF-1α and -2α genes in a hypoxia-sensitive teleost species (Megalobrama amblycephala): cDNA cloning, expression and different responses to hypoxia. Comp. Biochem. Physiol. B 157, 273–280.
Sollid, J., Nilsson, G.E., 2006. Plasticity of respiratory structures - adaptive remodeling of fish gills induced by ambient oxygen and temperature. Respir. Physiol. Neurobiol. 154, 241–251.
Sollid, J., De Angelis, P., Gundersen, K., Nilsson, G.E., 2003. Hypoxia induces adaptive and reversible gross morphological changes in crucian carp gills. J. Exp. Biol. 206, 3667–3673.
Sun, J.L., Zhao, L.L., Wu, H., Liu, Q., Liao, L., Luo, J., Lian, W.Q., Cui, C., Jin, L., Ma, J.D., Li, M.Z., Yang, S., 2020. Acute hypoxia changes the mode of glucose and lipid utilization in the liver of the largemouth bass (*Micropterus salmoides*). Sci. Total Environ. 713.
Sun, X., Tu, K., Li, L., Wu, B., Wu, L., Liu, Z., Zhou, L., Tian, J., Yang, A., 2021. Integrated transcriptome and metabolome analysis reveals molecular responses of the clams to acute hypoxia. Mar. Environ. Res. 168, 105317.
Tao, Y.F., Qiang, J., Bao, J.W., Chen, D.J., Yin, G.J., Xu, P., Zhu, H.J., 2018. Changes in physiological parameters, lipid metabolism, and expression of microRNAs in genetically improved farmed tilapia (Oreochromis niloticus) with fatty liver induced by a high-fat diet. Front. Physiol. 9, 1521.
Tristan, C., Shahani, N., Sedlak, T.W., Sawa, A., 2011. The diverse functions of GAPDH: views from different subcellular compartments. Cell. Signal. 23, 317–323.
Wang, Z., Gerstein, M., Snyder, M., 2009. RNA-Seq: a revolutionary tool for transcriptomics. Nat. Rev. Genet. 10, 57–63.
Wang, M.L., Wang, W.D., Wang, J.S., Zhang, J., 2018. MiR-182 promotes glucose metabolism by upregulating hypoxia-inducible factor 1α in NSCLC cells. Biochem. Bioph. Res. Co. 504, 400–405.
Wen, X., Hu, Y.D., Zhang, X.Y., Wei, X.Z., Wang, T., Yin, S.W., 2019. Integrated application of multi-omics provides insights into cold stress responses in pufferfish Takifugu fasciatus. BMC Genomics 20.
Wen, M., Zhang, Y.X., Wang, S.Y., Li, Q., Peng, L.Y., Li, Q.L., Hu, X.J., Zhao, Y.L., Qin, Q. B., Tao, M., Zhang, C., Luo, K.K., Zhao, R.R., Wang, S., Hu, F.Z., Liu, Q.F., Wang, Y. D., Tang, C.C., Liu, S.J., 2022. Exogenous paternal mitochondria rescue hybrid incompatibility and the destiny of exogenous mitochondria. Reproduction and Breeding. 2, 83–88.
Wu, C.B., Liu, Z.Y., Li, F.G., Chen, J., Jiang, X.Y., Zou, S.M., 2017. Gill remodeling in response to hypoxia and temperature occurs in the hypoxia sensitive blunt snout bream (Megalobrama amblycephala). Aquaculture 479, 479–486.
Wu, C.B., Zheng, G.D., Zhao, X.Y., Zhou, S., Zou, S.M., 2020. Hypoxia tolerance in a selectively bred F4 population of blunt snout bream (Megalobrama amblycephala) under hypoxic stress. Aquaculture 518, 734484.
Xiao, J., Kang, X.W., Xie, L.H., Qin, Q.B., He, Z.L., Hu, F.Z., Zhang, C., Zhao, R.R., Wang, J., Luo, K.K., Liu, Y., Liu, S.J., 2014. The fertility of the hybrid lineage derived from female Megalobrama amblycephala×male Culter alburnus. Anim. Reprod. Sci. 151, 61–70.
Zhang, W., Cao, Z.D., Fu, S.J., 2012. The effects of dissolved oxygen levels on the metabolic interaction between digestion and locomotion in cyprinid fishes with different locomotive and digestive performances. J. Comp. Physiol. B. 182, 641–650.
Zhu, C.D., Wang, Z.H., Yan, B.A., 2013. Strategies for hypoxia adaptation in fish species: a review. J. Comp. Physiol. B. 183, 1005–1013.